Journal of
Marine Science
and Engineering

Article

Sequence Stratigraphy, Sedimentology, and Reservoir Characteristics of the Middle Cretaceous Mishrif Formation, South Iraq

Leifu Zhang, Wenqi Zhang *, Yong Li, Benbiao Song, Dawang Liu, Ya Deng, Jiacheng Xu and Yuning Wang

Research Institute of Petroleum Exploration and Development, China National Petroleum Corporation (CNPC), Beijing 100083, China; zhangleifu@petrochina.com.cn (L.Z.); songbenbiao@petrochina.com.cn (B.S.); liudawang@petrochina.com.cn (D.L.); dengya@petrochina.com.cn (Y.D.); xujiacheng@petrochina.com.cn (J.X.); wangyuning@petrochina.com.cn (Y.W.)
* Correspondence: zhangwenqi1982@petrochina.com.cn

Abstract: The Cenomanian–Early Turonian Mishrif Formation is a great contributor to oil production in Iraq. Integrating petrographic, mineralogical, and wireline logging data from 52 wells, this study provides an improved understanding of the sequence stratigraphy, depositional evolution, and reservoir characteristics of the Mishrif Formation in the Mesopotamian Basin, south Iraq. Five types of facies associations are classified: lagoon, shoal, rudist bioherm, shallow marine, and deep marine. Such a classification allows convenient differentiation and interpretation of wireline logs. A sequence stratigraphic framework including five third-order sequences (Mhf 1 to Mhf 5) for the Mishrif Formation is established mainly using wireline logging data of close-distance wells, with the aid of cores and thin sections. Two end-member depositional evolution stages are recognized, from clinoform-like progradational shoal complexes in Mhf 1 within a shallow marine environment, to tidal channels in Mhf 2–3 within a lagoon environment. For Mhf 4–5, abrupt changes in facies associations from north to south indicate the development of an intra-shelf basin where organic-rich mudstones directly overlie the shallow marine grainstone shoals and lagoonal wackestones. Reservoir characteristics and compartmentalization are directly controlled by the sequence stratigraphic framework. Sequence boundaries are featured by wackestones and mudstones overprinted by cementation; they are regionally correlatable and work as regional barriers. Shoal complexes in Mhf 1 and tidal channels in Mhf 2–3 are the main reservoir units. Mudstones and wackestones are intra-reservoir baffles and become more frequently developed towards the south, reflecting the increasing water depth towards south. The characterization of the tidal channels, clinoform-like shoals, and intrashelf basinal deposits in the current study could benefit later development of the Mishrif Formation.

Keywords: Mishrif Formation; Mesopotamian Basin; sequence stratigraphy; reservoir potential; intra-shelf basin; tidal channel

Citation: Zhang, L.; Zhang, W.; Li, Y.; Song, B.; Liu, D.; Deng, Y.; Xu, J.; Wang, Y. Sequence Stratigraphy, Sedimentology, and Reservoir Characteristics of the Middle Cretaceous Mishrif Formation, South Iraq. *J. Mar. Sci. Eng.* **2023**, *11*, 1255. https://doi.org/10.3390/jmse11061255

Academic Editor: George Kontakiotis

Received: 11 May 2023
Revised: 29 May 2023
Accepted: 30 May 2023
Published: 20 June 2023

1. Introduction

Carbonate reservoirs in the Middle East hold considerable oil and gas reserves of the world. In Iraq, the Mishrif Formation of the Cenomanian–Early Turonian in the Mesopotamian Basin contains more than 30% of oil reserves [1], and is regarded as the most important reservoir in several world-class oilfields in southern Iraq, such as the West Qurna and Rumaila oilfields. Characterized by a general shallowing-upward pattern, the Mishrif Formation represents a stable deposition transitioned from an extensive shallow-marine carbonate platform into a lagoonal and supra-tidal environment [2,3]. The deposits are mainly bioclastic limestones, with local build-ups of algae and corals, and rudist bioherms during a ca. 3 million year period [4,5].

Facies associations, reservoir potentials, and depositional settings of the Mishrif Formation have been widely studied [3,6–9]. In addition, equivalent formations to the Mishrif

Formation elsewhere in the Middle East, including the Sarvak Formation of Iran and the Natih Formation of Oman, are also widespread and oil-proliferous in the Arabian Plate. The sequence stratigraphy and sedimentology of these equivalent formations are studied in detail, as is their great hydrocarbon potential [10,11]. However, using different datasets, different depositional models are proposed. While agreeing with the widespread development of rudist buildups, the depositional environment of the Mishrif Formation is still in debate (e.g., ramp, reef, and slope margin) [1,3,12–15].

To date, there are a large number of studies on the sequence stratigraphic frameworks of the Mishrif Formation, many of them focusing on one or a few fields. However, different sequence stratigraphic frameworks are proposed for the Mishrif Formation and its equivalent formations. Early studies with limited data tend to divide the Mishrif Formation into two third-order sequences, separated by an intra-formational unconformity recorded at Amara [15,16]. Using more well data, Refs. [3,8] proposed a scheme that classified the Mishrif Formation into three third-order sequences (S1, S2, and S3). Maximum Flooding Surface (MFS) within S2 and S3 is equivalent to the Middle Cenomanian MFS-130 proposed by [17] and the Late Cenomanian MFS-135 proposed by [1]. Ref. [6] integrated the core and well data of the H field in south Iraq, and classified the Mishrif Formation into six third-order sequences (SB-A to SB-F). For neighboring fields such as the West Qurna and Rumaila oilfields, three and five third-order sequences are proposed for the Mishrif Formation, respectively [18,19]. Different stratigraphy schemes result in uncertainties in terms of regional correlation and comparison of depositional units, also impeding reservoir characterizations and efficient oil and gas development.

Meanwhile, the Mishrif Formation is highly heterogeneous [7,18,20] and depositional facies can change rapidly both vertically and horizontally. For low-gradient carbonate systems such as the Mishrif Formation, a tubular geometry and "layer-cake" horizontal correlation is often applied [10]. For systems analogous to the Mishrif Formation, recent studies employing high-resolution outcrop characterization and seismic data revealed the existence of prograding clinoforms; in addition, that organic-rich intrashelf basins were formed at the time of the Mishrif deposition [10,21–24]. A diagenesis overprint can introduce additional heterogeneity. For example, vugular features can have a strong impact on porosity–permeability characteristics and the flow behavior of carbonate rocks. To accurately represent the flow behavior of vuggy carbonate rocks is essential yet challenging [25,26]. Meteoric, burial, and tectonic-related cementation could significantly decrease the reservoir quality [8,27]. The heterogeneity of the Mishrif Formation in southern Iraq can also be demonstrated by the different production behaviors in neighboring oilfields, for instance, the West Qurna and Rumaila oilfields.

The objectives of this work, therefore, are to (1) investigate the depositional evolution and facies association of the Mishrif Formation in southern Iraq; (2) establish a sequence stratigraphic framework for the Mishrif Formation that allows for regional correlation; (3) unravel the internal heterogeneity such as distribution of clinoforms, tidal channels, and intrashelf basin deposits, as well as reservoir architectures for exploration and production purposes.

2. Geological Setting

The study area in southern Iraq is located in the southern Mesopotamian Basin (Figure 1A), which is an asymmetric foredeep extending from northern Iraq to the Arabian Gulf [1]). The northeastern margin of the basin is bounded by the Zagros Mountains and a series of folded zones, the western margin is bounded by the Mesozoic stable shelf [1]. From the Jurassic to late Cretaceous, along the passive margin of the Neo-Tethys Ocean and the Arabian Plate, the Mesopotamian Basin is characterized by development of a series of shallow intra-shelf basins, for example the Najaf Intra-Shelf Basin/Rumaila Intra-Shelf Basin [28]. In the late Cretaceous, the collision of the Arabian plate and Eurasia Plate resulted in the development of northwest–southeast trending foredeep. Since the late Paleogene, renewed continental convergence formed the Zagros Orogeny characterized by a series of compressional folds and faults in the Zagros fold belt, also resulting in the closure of the Neo-Tethys Ocean [28]. By contrast, the study area is less affected by the compression, but a series of north–south trend folds were developed, perhaps caused by salt diapirism [1,3]. Two oilfields in the study area reflect a present day long-axis north–south trend asymmetrical anticline, with the western flank slightly deeper than the eastern flank and a regional saddle separates the oilfield into north and south regions [2].

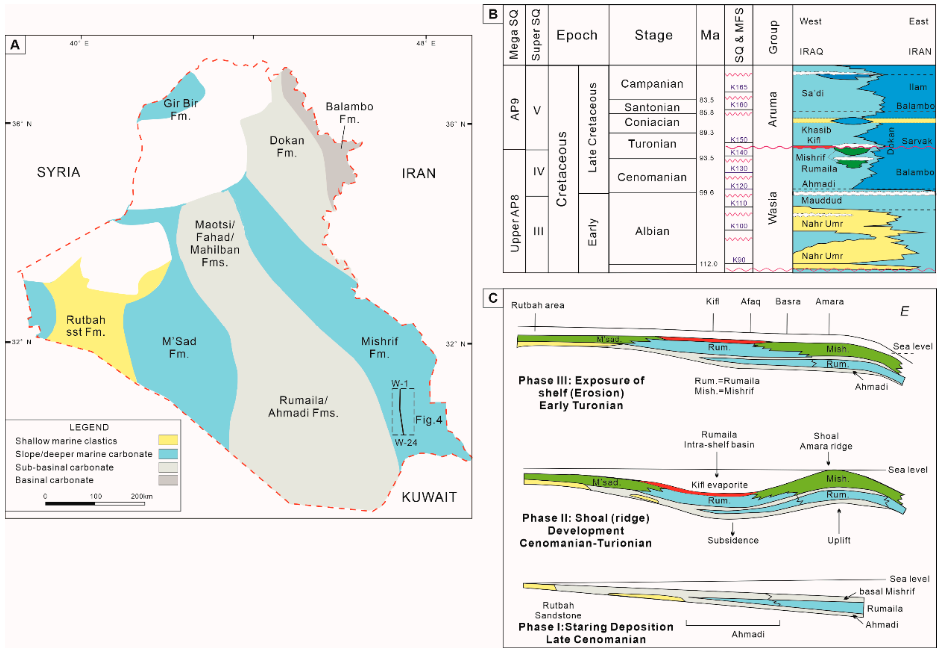

Figure 1. (**A**) Latest Albian–Early Turonian paleogeography map of Iraq, modified from [1]; (**B**) Chronostratigraphy of Iraq and Iran, modified from [1], mega-sequence and super-sequence are from [17]); (**C**) Schematic section showing geological evolution of the Cenomanian–Early Turonian of south Iraq, modified from [1,29].

The Mishrif Formation, firstly described from the Zubair-3 Well in south Iraq, is regarded as being developed in Mid-Cenomanian to Early Turonian based on paleontological studies [3]. It was classified into Supersequence IV within the Megasequence AP8 by [1,17], representing a transition from onlap margin to basin (Figure 1B). The formation is 350 to 400 m thick in the Amara/Buzurgan/Majnoon area and thins towards the southwest, being less than 10 m thick at the Safawi-1 well near the border to Saudi Arabia [1,15].

The evolution of the Mishrif Formation can be divided into three major phases (Figure 1C, [1,29]). The first phase is the start of the deposition: the Rutbah Sandstone in the west and the Ahmadi shales in the east were firstly developed as an east-deepening monocline. Then, shelf carbonates of the M'sad Formation in the west and the Ahmadi–Rumaila formations were developed. Overlying the Rumaila Formation, deposition of the basal Mishrif Formation was initiated. The second phase is the growing shoal/ridges: the Rumaila Formation graded into the Mishrif Formation towards the east and north, while the Mishrif Formation underwent fast deposition due to a combination of sea level fall and tectonic uplift (Figure 1C). Consequently, shoals and ridges were developed and gradually graded to M'sad Formation in the west and Dokan and Balambo Formation in the northeast. Meanwhile, the Rumaila Intra-shelf Basin was initiated, depositing lime mudstones and organic-rich shales of the Rumaila Formation during highstand, and evaporite of the Kifl Formation during lowstand, respectively. The third phase is the exposure of the shelf (erosion): due to the quiescence of tectonic subsidence and uplift as well as sea level fall, the Mishrif Formation underwent subaerial exposure, and graded westwards into shelf carbonates of the Rumaila Formation, evaporite of the Kifl Formation, and the shallow marine carbonates of the M'sad Formation. The termination of the Mishrif deposition associated with subaerial exposure was accompanied by a regional unconformity. The top of the Mishrif Formation can be well differentiated from the overlying

Khasib Formation shales resulting from a rapid flooding (Figure 1B, Figure 2). The Mishrif Formation is time-equivalent and correlatable with the Sarvak Formation of Iran and the Natih Formation of Oman, which have been studied in detail [10,30].

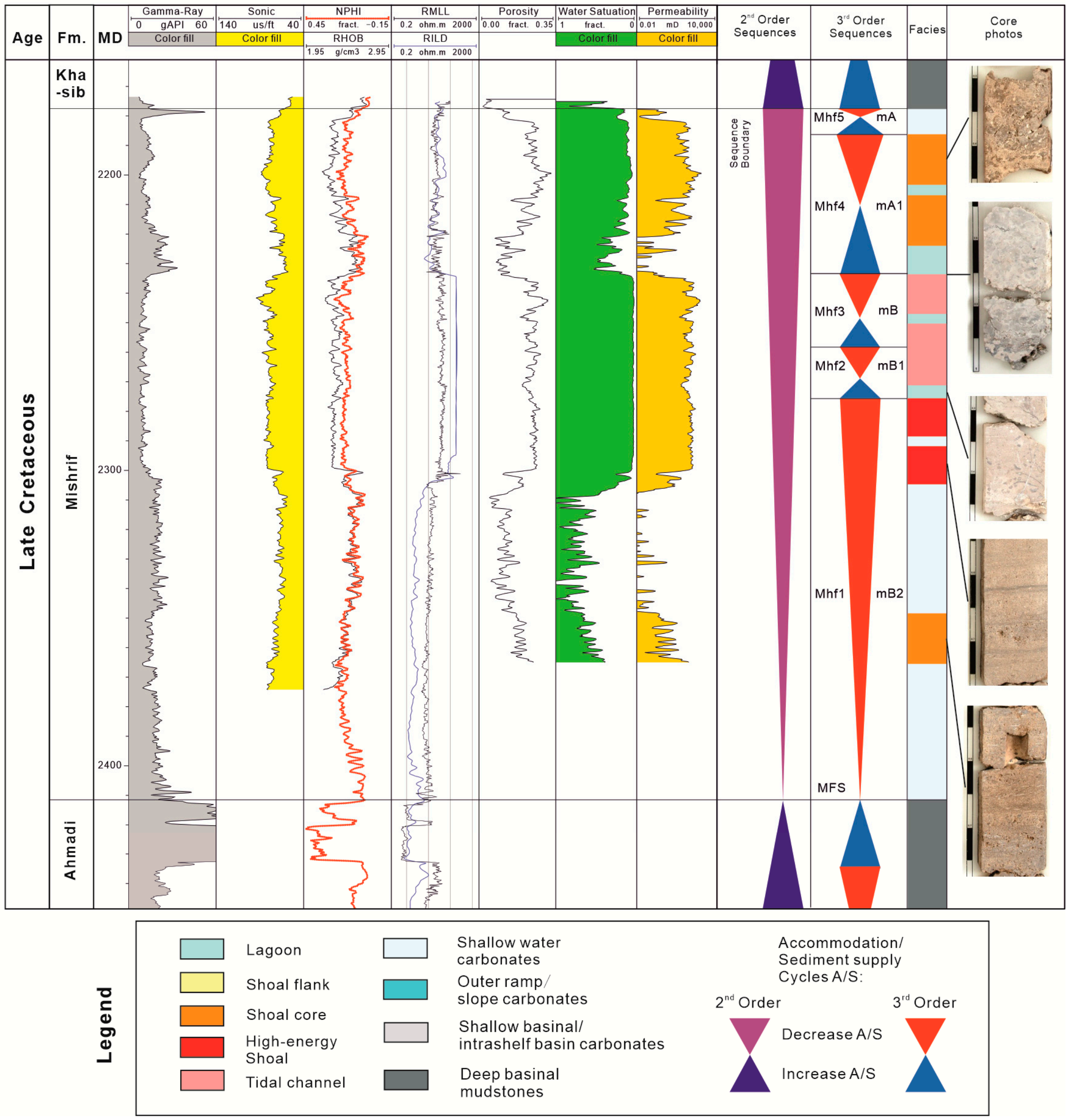

Figure 2. Composite log display of a typical cored well W19, with interpretation of sedimentary facies and sequence stratigraphy.

3. Materials and Methods

More than 2000 thin sections, 200 m thick continuous cores, and wireline logs from more than 50 wells were used in this study. Thin section samples were analyzed using a polarizing microscope, many of them were stained using Alizarin Red S to differentiate the dolomite from calcium carbonate. Petrographic characterizations follow the classification schemes of [31], based on the depositional textures. Sequence stratigraphy framework relies on the identification of the maximum flooding surface (MFS), and transgressive–regressive sequences in the Mishrif Formation were interpreted following the methods and terminology of [32]. They reflect the change in accommodation and sediment supply ratio (A/S ratio). The regional sequence stratigraphy framework for the Arabian Plate provided by [4,17] was also used to support the current correlations.

Lithologies and biofacies generally have a good match to wireline log data of wells, allowing log-based definition of sequence stratigraphic framework. In this study, logs of Gamma-ray (GR), acoustic (DT), thermal neutron porosity (NPHI), bulk density (RHOB), and resistivity (e.g., ILD) were utilized. They are the critical data which support the interpretation of facies association, sequence stratigraphy, and depositional evolution. Along the north–south direction, 52 wells are carefully correlated for this purpose (e.g., Figure 2). Some of the wells are so close and bear similar logging characteristics; thus, only a few representative wells are chosen for the purpose of better showing the internal reservoir characteristics. Consequently, a cross-section comprising 24 wells (W1 to W24 in Figure 1) is established and presented.

4. Results

Sedimentological characterizations based on the integration of wireline logs, cores, and thin sections from 52 wells have led to the identification of 5 facies associations: lagoon, shoal, rudist biostrome, shallow marine, and deep marine. Interpretations of microfacies is beyond the scope of this study, since the main objective is to understand the variations in facies associations under a large-scale sequence stratigraphic framework. Typical characteristics of each facies associations are explained as follows.

4.1. Reservoir Sedimentological Characteristics

4.1.1. Lagoon

Mud-rich wackestones, and rare packstones with abundant benthic foraminifera, ostracods, and gastropods are representative products of this facies association. Miliolids are the most common benthic foraminifera (Figure 3a), whereas rudist debris is scarce. Common bioturbations can be observed on cores (Figure 3a), the abundance of miliolids, muddy texture, and low-diversity of faunas in the thin sections suggest a low energy lagoonal environment. In terms of wireline loggings, high gamma-ray reading and low porosity and sonic motifs (Figure 2) are characteristic of lagoonal facies, yet the gamma ray responses are not as high as the deep marine facies, suggesting the lagoon facies are perhaps not as intensively restricted. The frequent existence of tidal channels that entered the lagoon from the marine-side and deposited high-energy grainstones also demonstrates that the lagoons are not highly restricted. Landwards of the lagoon, tidal flat facies are represented by wackestones, lime mudstones with rare biocomponents. Brecciation and dissolution features observed on cores suggest local exposure, which is characterized by an abrupt peak of gamma ray and sonic logs (Figures 2 and 3g). Tidal flat facies are generally associated with lagoon facies and limited to the top of the Mishrif Formation; therefore, they are not specifically discussed and are incorporated into lagoonal facies.

Lagoon facies association is mainly developed at the top of the Mishrif Formation. From north to south, the distribution of this facies association is less abundant (Figure 4). Tidal channels are frequently observed in the northern area, whereas they abruptly diminish towards the south (near W18 in Figure 4). This perhaps marks the transition of the lagoon environment to shallow marine facies.

4.1.2. Shallow Marine

Massive, thick, fine-sized wackestones to packstones with a variety of bioclasts including rudest, green algae, echinoderms, bivalves, and foraminifera (Figure 3b) represent the shallow marine facies. Shallow marine in this study is the setting between fair-weather wave base and storm wave base. Hence, the mid-ramp, outer ramp, platform slope facies used elsewhere [7] are also considered as a part of shallow marine facies association. Leaching and dissolution are rarely observed for this facies association. Shallow marine facies are predominant in the study area especially during early deposition of the Mishrif Formation. In vertical profile, it works as “background” facies encasing several individual shoal bodies.

Laterally, it is rudist-rich and grain-rich in the north yet becomes wackestone-dominant towards the south (Figure 4).

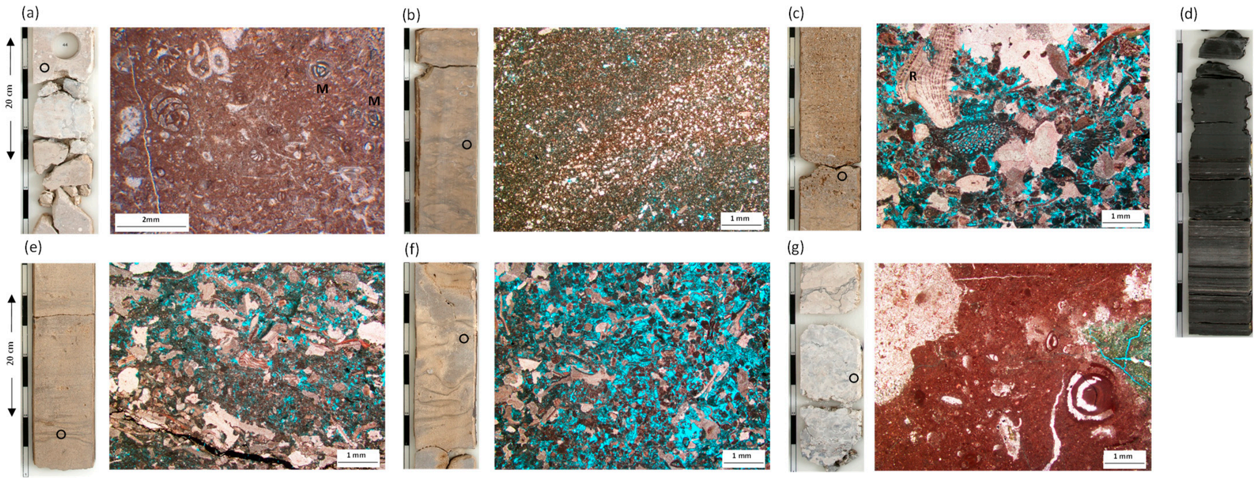

Figure 3. Core photographs and photomicrographs of some of the facies associations of the Mishrif Formation. (**a**) Lagoon facies, W19 Well, 2227.84 m, within Mhf 3; photomicrograph shows typical benthic foraminifera miliolid (M); (**b**) Shallow marine/mid-ramp facies, core shows abundant bioturbation and bivalves fragments and debris, W19 Well, 2303.24 m, within Mhf1; photomicrograph show equant calcite cementation; (**c**) Rudist biostrome facies, W19 Well, 2289.43 m, within Mhf1, core and photomicrograph both show rudist fragments (R); (**d**) Deep-marine facies black shales with good horizontal lamination, W18 Well, 2299.5 m, suggesting restricted, low-energy environment; (**e**) Shoal facies packstone–grainstone, R1 Well, 2292.86 m, within Mhf1, medium-coarse abraded rudist bioclasts, common leaching, and local fracturing; (**f**) Back-shoal facies packstone–grainstone, W19 Well, 2271.83 m, within Mhf2, boring traces on cores and abundant peloids, recrystallized rudist and mollusk bioclasts on photomicrographs; (**g**) Characteristics of the sequence boundary (top Mhf3, mB), W19 Well, 2222.05 m.

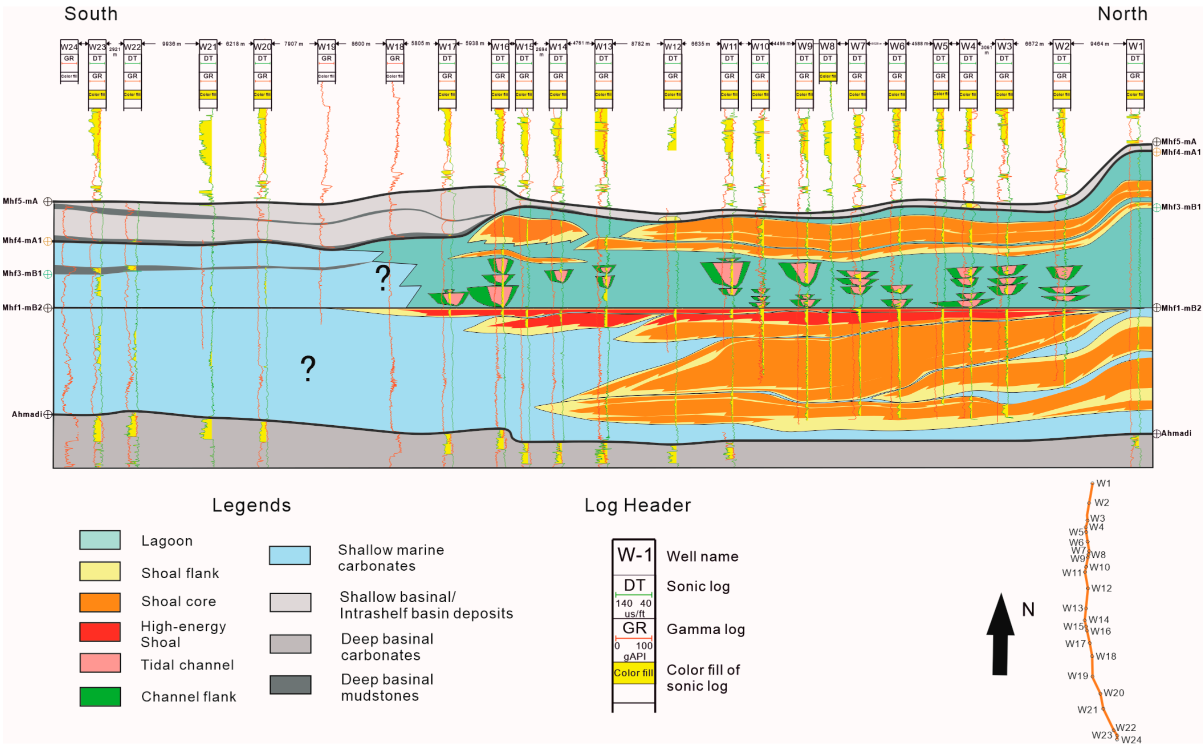

Figure 4. North–south correlation of 24 wells with detailed interpretation of facies associations within a sequence stratigraphic framework. Correlation line as shown in Figure 1A.

4.1.3. Shoal

Grainstones and skeletal–peloidal packstones represent the deposits of shoal facies. On cores, thin bedded laminations can be observed with abundant bioclast and bioturbation; in addition, leaching and local fracturing appear (Figure 3e). Medium-coarse abraded rudist bioclasts, peloids, and skeletal grains of echinoderms, and gastropods are key biocomponents (Figure 3e). The depositional environment of shoals is characterized by relatively shallow and moderate- to high-energy conditions; thus, local shoal build-ups could be re-worked by occasional storms or tidal activities. The co-occurrence of leaching and dissolution, micritization and bioturbation, suggest that shoal facies are developed in a variable environment. Meanwhile, shoal facies are considered as being deposited above a fair-weather wave base, the content of mud is therefore very low, resulting in low-value and blocky gamma-ray logs (Figure 2). In contrast, high, blocky sonic logs suggest good reservoir quality.

Shoals are developed in both the basal and upper part of the Mishrif Formation. At least six rudist-bearing shoals are depicted in the basal part, with thickness ranging from ~5 m to ~40 m, displaying a prograding clinoform feature (Figure 4). Four shoals are depicted at the upper part. The prograding feature is not obvious; one shoal body near W16 is relatively mound-like and has a limited lateral extent (~200 m). They are likely associated with the development of intra-shelf basins.

Behind shoals or rudist build-ups towards the lagoon, back shoal facies are developed and characterized by wackestones and packstones, suggesting a low-moderate environment separating high-energy shoals and low-energy lagoons. Chondrodonta, bivalves, foraminifera, and local rudist fragments are the main biocomponents (Figure 3f). Back-shoal facies are generally associated with shoals; however, it is not easy to differentiate each other on well logs. They are, therefore, not independently discussed in this study. Instead, shoal flank and shoal core are applied, with the latter having higher porosity readings.

4.1.4. Rudist Biostrome

Radiolitid rudist shells with fragments built up an in-situ framework, which can trap sediment and angular bioclasts such as fragmented rudist shells in its interspaces, forming the rudist biostrome in a very shallow, high-energy setting (Figure 3c). Those rudist fragments are generally broken by high-energy water, leaving a poorly sorted texture. Adjacent to shoals, towards the shallow sea, rudist biostrome is locally developed but not as extensive as those rudist-rich build-ups in slope and shoal locations (Mahdi et al., 2013). It is noteworthy that it is difficult to interpret and map the pure rudist biostrome based on well logging data, an accurate identification requires high-resolution three-dimensional seismic characterizations. Because of the erosion and reworking, true rudistid reefs (framestones, floatstones, and boundstones) are rarely encountered [9] and might be re-deposited as "tabular reef" [33].

4.1.5. Deep Marine

This facies association is represented by black shales (Figure 3d). Apparent horizontal laminations suggest a suspension-fallout in a quiet, restricted deep-sea environment without influence of clastic influx or carbonate production. In this study, such black shales only occur at the top of the Mishrif Formation, characterized by abnormally high gamma ray peaks. This shale interval is equivalent with the basinal Khasib Shale as described in [3,8], overlying the Khasib-Mishrif Unconformity. In the southern part of the study area, similar high gamma peaks appear in the upper part of the Mishrif Formation and are considered as sequence boundaries.

The Ahmadi shales and Khasib shales are regionally comparable; they are key surfaces in terms of sequence stratigraphy and hence defined by regional studies such as MFS K120 and K140, respectively [1,17]. Meanwhile, they provide important regional seals for the Mishrif Formation and the Mauddud Formation [34]. The Ahmadi shales and its coeval Shilaif Formation, have decent total organic carbon (TOC) and are an important source of rocks [34,35]. The Khasib shales are perhaps deposited in a restricted environment and grade into marls and marly limestone upwards [34]. Such shales have similar characteristics to shales described elsewhere [36,37]; they perhaps have unconventional reservoir potential but are beyond the scope of the current work.

4.2. Sequence Stratigraphy

The Cenomanian–Turonian Mishrif Formation in Southern Iraq belongs to the upper part of the Arabian Plate megasequence AP8 and supersequence IV as proposed by [1,17]. The unconformity at the top Mishrif Formation forms the boundary of megasequence AP8 and AP7. K140 is the maximum flooding surface (MFS) beneath this unconformity and K120 is the MFS above the Ahmadi Formation [17]. Supersequence IV can be classified into several smaller-order cycles, yet such classifications appear to be a case-by-case scenario varying by different study area and different authors. A chronostratigraphy was established for the study area based on foraminifera, and several different stratigraphic frameworks exist [3,6,8,38].

In this study, five third-order sequences are interpreted for the Mishrif Formation; each third-order sequence is composed of a transgressive and a regressive cycle with the maximum flooding surface (MFS) as the boundary, reflecting the change in accommodation and sediment supply ratio (A/S ratio). From base to top, five third-order sequences are named Mhf 1, Mhf 2, Mhf 3, Mhf 4, and Mhf 5. Within each third-order sequence, the regressive cycle is generally larger than the transgressive cycle. The exception is Mhf 1, only its regressive cycle is within the Mishrif Formation whereas its transgressive cycle is equivalent to the underlying Rumaila Formation (Figure 2) and hence beyond the scope of this study. A high-resolution regional correlation has been carried out in this work based on the integration of well, cores, and petrophysical data, allowing for investigation of the depositional evolution and reservoir architecture.

4.2.1. Sequence Mhf 1

This is the lowermost sequence interpreted in the Mishrif Formation within the study area. The Mhf 1 sequence comprises the lowermost part of the Mishrif Formation and a part of the Rumaila–Ahmadi Formation. Only the regressive cycle of Mhf 1 appears in the Mishrif Formation, the transgressive cycle lies within the underlying Rumaila Formation to Ahmadi Formation [1]. The Rumaila Formation is characterized by "oligosteginal"/sub-basinal carbonates and gradually grades into the underlying Ahmadi Formation; however, the boundary between the Mishrif Formation and the Rumaila Formation cannot be accurately determined in this study. The base of the Mhf 1 is picked at the Ahmadi Formation featured by a transition to a high, blocky gamma-ray interval (Figure 2). The top of Mhf 1 is consistent with the "Disconformity" defined by [3,8]. Additionally, the top Mhf 1 is also consistent with the top of mB2, the lower part of mB, which is widely used by the petroleum industry [33].

The Mhf 1 is becoming thinner from north to south, with an abrupt change in the middle region. Sonic logs (DT) can adequately reflect porosity and reservoir potential, together with gamma-ray logs (GR), could help predict the reservoir distribution. In the north, a majority of the Mhf 1 is stacked shoal complexes with high DT values and low GR values (Figures 2 and 4). By contrast, in the south, few to no shoals appear, while shallow marine facies are predominating. Although a few high-DT value intervals occur locally, the high, serrated to block GR values suggest the shallow marine environment. A low value, blocky motif of GR logged in the north gradually changes to higher value, serrated-blocky motifs in the south, suggesting the water column is thickening towards the south.

A high-resolution well correlation (Figure 4) depicts that at least six rudist-bearing shoals are developed in the Mhf 1. They are likely extensions of the five build-ups interpreted by [33] in this interval. The stacking of grainstone shoals display a north to south progradation pattern, perhaps clinoforms pinching out within a shallow-marine environment [8]. These clinoforms may be comparable with the time-equivalent intervals elsewhere in the Arabian Plate, such as the Savark Formation and the Natih Formation [22,38]. A thin (c.a. 5 m thick) grainstone shoal at the uppermost part of the Mhf 1, featured with low GR and high porosity and sonic values, represents the most favorable reservoir. The top of the Mhf 1 sequence is characterized by subaerial exposure in the north and hardground in the south. Due to exposure, vuggy pores suggesting later dissolution further improve the reservoir quality, making the topmost shoal the highest permeable zones in the Mhf 1.

4.2.2. Sequence Mhf 2

The depositional environment changed drastically after Mhf 1. Overlying the shallow marine-dominated Mhf 1, the Mhf 2 sequence is dominated by peri-tidal lagoonal deposits of wackestones with abundant bioturbation, suggesting a significant sea-level fall compared with Mhf 1. Within the lagoonal background, tidal channels are frequently developed, featured with a channeling-upward pattern (Figure 4): gamma-ray logs display an upward-decrease motif, whereas sonic logs display an upward-increase pattern. This channel-upward pattern is the critical means of interpreting tidal channels in this study since no seismic data are available. Once a tidal channel is interpreted in a certain well, it is carefully correlated with its adjacent wells. Well correlations demonstrate that tidal channels generally cannot extend laterally more than 500 m, which in turn proves that these are meandering tidal channels, rather than the grainstone shoals interpreted by [3,8]. The north–south trend cross-section (Figure 4) is therefore likely perpendicular with the paleoflow direction of the tidal channels. Skeletal shoals or mounds might develop locally (e.g., W14), judging from the occasional shoaling-upward pattern based on logs.

Tidal channels form an important reservoir unit in lagoon-dominated Mhf 2. Well correlation displays a poor inter-channel connectivity. Instead, they form local high-permeability zones and are of great importance in terms of oil development [39]. Towards the south, the Mhf 2 maintains an overall stable thickness but lagoonal facies gradually grade into shallow marine facies/possibly mid-outer ramp facies. This deepening-south trend maintains in the Mhf 3 sequence.

4.2.3. Sequence Mhf 3

The deposition of peritidal lagoonal wackestones and tidal channel grainstones in Mhf 3 demonstrates a similar environment with that of Mhf 2. On the correlation panel based on well logs, tidal channels, featured with a typical channeling-upward/ thinning-upward pattern, are frequently observed within Mhf 3 (Figure 4). Unlike the stable depositional environment of the Mhf 1 in the entire study area, the paleo-environment of Mhf 2 and Mhf 3 clearly changes from the northern to southern region. A small-scale shoal/skeletal build-up is interpreted within the regressive cycle, at the top of Mhf 3, at the middle region of the study area (well 11–12), marking the transition of lagoonal facies to shoal/back-shoal facies, and to mid-outer ramp facies within deeper water depth (Figure 4).

The boundary of Mhf 2 and Mhf 3 appears subtle in the north; however, it becomes apparent by the occurrence of organic-rich mudstones with abnormally high gamma-ray peaks. The top of Mhf 3 is characterized by a series of exposure surfaces in the northern region (Figure 2), supported by the occurrence of microbialite, iron staining in thin sections, and exposure surfaces with karstification features, such as karst pipes in cores (Figure 3g). Additionally, this sequence boundary is highly cemented giving rise to a regional cap-rock.

4.2.4. Sequence Mhf 4

After the exposure of the Mhf 3 sequence boundary, deposition of thick shoals and bioclastic build-ups suggest a flooding and paleo-environment changed from tidal lagoon to shallow marine facies again. In the northern region of the study area, at least two shoal complexes are recognized, featured with upward-increasing high sonic values and low GR values on logs, as well as cross-laminated grainstones with rudist fragments and echinoderms on cores (Figure 2). An abrupt transition occurs at the middle of the study area near well 12 (Figure 4), where large-scale shoals shift to two narrow but thick build-ups, and to shallow marine carbonates to the south (Figure 4). In the southern region of the study area, the transgressive cycle of Mhf 4 is characterized by rapid flooding culminating in the deposition of organic-rich shales, the abrupt change from north to south perhaps marks a transition from a shallower inner ramp, via a rimmed margin to a deeper intra-platform basin.

4.2.5. Sequence Mhf 5

The Mhf 5 sequence is the last third-order sequence within the Mishrif Formation. The top of the Mhf 5 sequence is beneath the unconformity of the top Mishrif Formation (Khasib-Mishrif Unconformity in [8]). Above the unconformity, the Khasib deepwater shales are deposited.

This sequence is generally less than 10m thick in the north of the study area, characterized by low DT values and high GR values. In the northern region of the study area, the transgressive cycle is represented by a gradual increase in GR logs. Towards the southern region, this sequence becomes much thicker (>40 m), the transgressive cycle is reflected by several high GR peaks together with low sonic signatures within this sequence (Figure 4). Organic-rich wackestones and mudstones are deposited, perhaps resulting from deposition within the intra-shelf basin (Rumaila Basin or Najaf Basin, Figure 1B). The regressive cycle is accompanied by a few local build-ups in the north and a decrease in GR values in the south.

A positive carbon excursion is observed in this interval, suggesting that it is a part of the Oceanic Anoxic Event OAE2. The MFS within this sequence is likely consistent with K140 proposed by [4].

5. Discussion

5.1. Depositional Model

The Mishrif Formation in the Arabian Plate has been widely studied, and different depositional models have been proposed. Ref. [12] focused on the importance of rudist build-ups and classified the Mishrif Formation into sub-basinal slope margin, shallow outer reef margin, rudist reef, back-reef, and off-reef. The low-relief feature of the depositional environment was highlighted and was considered similar to ramp. Refs. [1,15] further determined the overall depositional environment as ramp. A shallow marine platform interior and a deep marine mid-outer ramp was identified. Microfacies include shoal, rudist biostrome, lagoon, tidal, mid-ramp, outer-ramp, and deep marine. Refs. [3,8] applied the concept of fair-weather wave base and storm wave base, and used them as criteria to determine the overall shallow open marine environment, rather than ramp. Towards the deep ocean, seven principal facies associations were sequentially recognized, including tidal flat, lagoon, back-shoal, shoal, rudist biostrome, shallow open marine, and deep marine [1,3,8]. In addition, the Natih Formation in Oman, time-equivalent to the Mishrif Formation, was interpreted as inner-ramp, mid-ramp, outer-ramp, and basin interior facies [24,30]. Despite differences in microfacies classification, published studies tend to agree that the Mishrif Formation was deposited within a shallow, low-relief (flat) carbonate platform primarily controlled by relative sea level change.

In this study, wireline logs are the key to unraveling the depositional evolution. Nevertheless, wireline log interpretations are somewhat subjective and, in some cases, cannot differentiate certain microfacies. Therefore, the overall depositional evolution within the entire Mishrif Formation is the focus, rather than the detailed characterization of microfacies. Despite an overall shallowing-upward trend for the Mishrif Formation being commonly agreed [3,8,15], pronounced facies changes resulting from changes in depositional environment are observed in this work. Herein, the well correlation suggests two shallowing phases within an overall shallowing-upward cycle. The first shallowing starts from the basal deep-marine Mhf 1, to shallow marine Mhf 2, to tidal-lagoon facies-dominated Mhf 3. Then, a short-term shallow marine flooding occurs in Mhf 4 but becomes shallower rapidly for the Mhf 5, where subaerial exposure and tidal flat-terrestrial facies occurs. Two end-members represented by Mhf 1 and Mhf 3, respectively, are highlighted according to log-based well correlation (Figure 5): shallow open marine with platform-top grainstone shoals, and shallow open marine with lagoonal tidal channels.

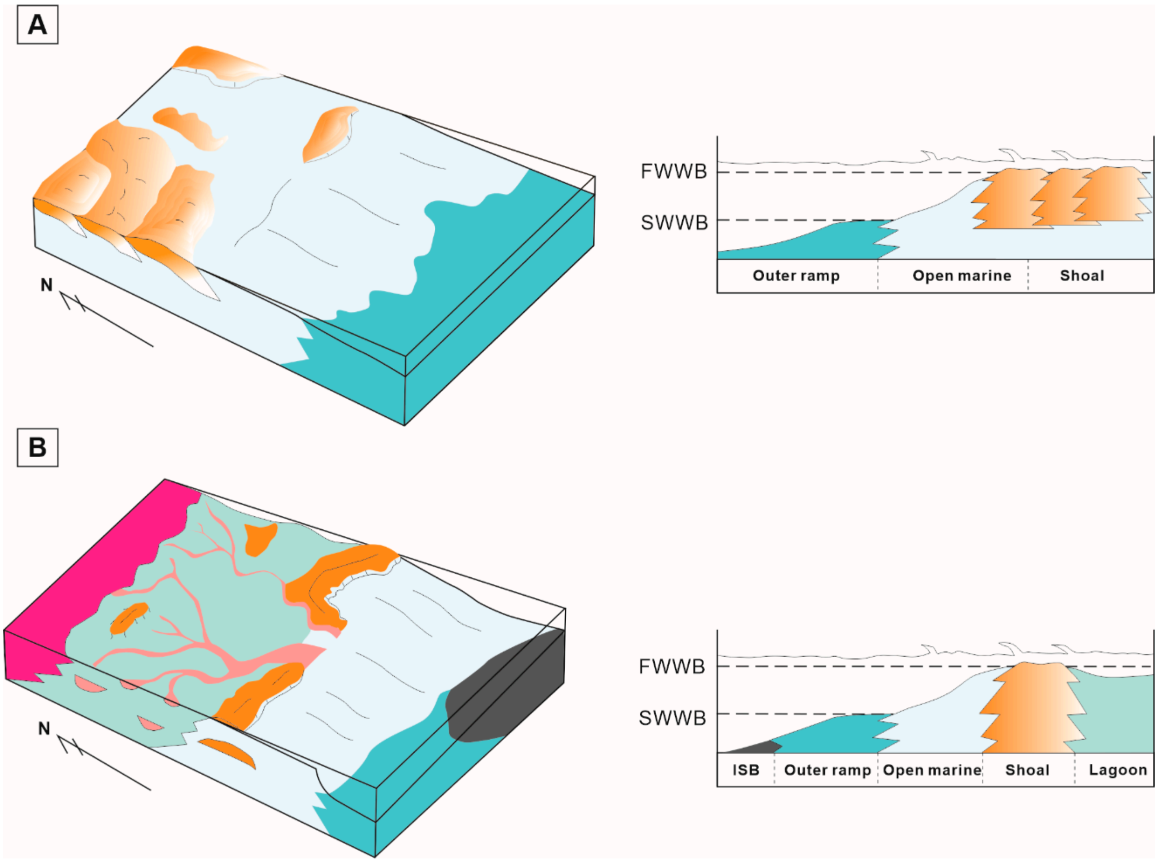

Figure 5. Schematic depositional model for two end-members. (**A**) Shallow open marine with grainstone shoals in Mhf 1; (**B**) Shallow open marine with lagoonal tidal channels in Mhf 3. ISB = Intrashelf basin.

5.1.1. Clinoform-Like Shoal Complex

The overall thickness of the regressive cycle of the Mhf 1 is relatively stable (~100 m, Figure 2). From north to south, however, the sedimentary facies change drastically. Shoals prograde from north to south, a clear progradation pattern appears on the north–south well correlation panel. From the top of Ahmadi Formation to the top of the Mhf 1 sequence boundary, careful correlation using the top of Mhf 1 as datum reveals the stacking of six shoal complexes (Figure 4). The stacking of these shoals displays an apparent prograding pattern, typical characteristic of clinoforms (Figures 5 and 6). Carbonate clinoforms are discovered based on seismic data and the outcrop of Cretaceous epeiric carbonate platform in the Middle East. Examples include outcrop characterization and modeling of Natih E Member in Oman [21], and high-resolution seismic subsurface studies of UAE and Oman [10,22]; they revealed complicated stratigraphic architectures of prograding clinoforms delineating platform margins and stated that clinoform geobodies are more complicated than a simple layer-cake model. Complex clinoform models must be considered in both static and dynamic reservoir modelling workflows so that proper rock properties are reproduced [21]. At the basal part of the Mishrif Formation in south Iraq, clinoform-like shoal complexes are recognized only on the basis of close-distance wells in this study (Figures 4 and 6); hence, unravel the detailed internal stacking characteristics within the fore-reef or shallow marine environments discussed elsewhere [3,15].

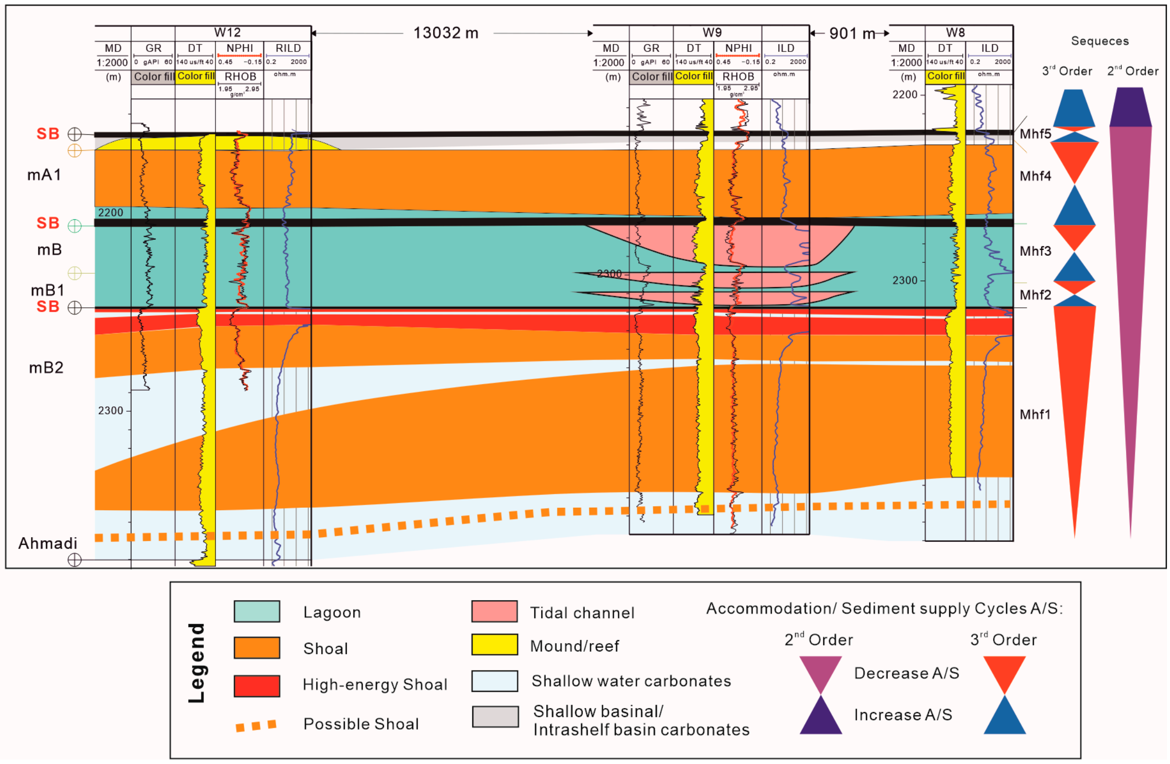

Figure 6. Correlation of W8, W9, and W12 showing prograding clinoform-like shoal complexes in the sequence Mhf 1, tidal channels in Mhf 2 and Mhf 3, isolated shoal complex in Mhf 4, and local mound/reef in Mhf 5. Sequence boundary (SB) is highlighted in black.

Assuming that sonic logs positively correlate with reservoir quality, the closer to the Mhf 1 top surface, the thinner the shoal complex, and the better the reservoir quality. The mechanism for this is perhaps an integrated control of sedimentology and diagenesis [40,41]. First, the continuous sea level fall suggests higher hydrodynamic conditions so that finer grains are elutriated. Second, subaerial exposure of the sequence boundary (Mhf 1 top) made the topmost shoal complex subject to meteoric water dissolution, creating vugs and pipes which improve porosity and permeability. The water depth increases towards the south, and sedimentation is dominated by shallow open marine environment, resulting in deposition of wackestones–packstones. Gamma-ray (GR) values are generally higher in the south (e.g., well 12–15, Figure 4), possibly suggesting a higher proportion of mud and the presence of intercalating mudstone layers; however, further core data are required to assist such an explanation.

The shallowing-upward is depicted by the occurrence of lagoonal facies in Mhf 2 and Mhf 3, suggesting a significant sea-level fall. Large-scale prograding shoal complexes are not developed there, only local rudist/reefal build-ups are developed at the platform margin. Towards the south, lagoonal facies grades into shallow marine facies, with the development of local shoal/build-ups at the margin. At Mhf 3 top, shale beds are developed and become thicker towards the south (Figure 4, Figure 6), reflected by a gamma-ray peak. By contrast, neither shale beds nor local grain-stone build-ups are interpreted on the Mhf 2 top. This implies a possible abrupt lagoon-shallow marine break was developed during the end phase of a regressive cycle of Mhf 2, perhaps related to tectonic movement as Amara paleohigh [1,15]. Tidal channels are frequently developed within the lagoonal facies, based on the typical "channel-upward" motifs on gamma ray and sonic logs.

5.1.2. Tidal Channel

A unique depositional unit in this study is the tidal channels developed within the tidal-lagoon environment. It is of great reservoir potential since grainstones in such channels act as high permeability zones in the upper reservoir unit (Mhf 2–3). A rare high-resolution outcrop characterization of the Natih Formation in Oman suggests that the outcropped tidal channels are generally 0.5–1 km wide, 2–5 m deep, and less than 30 km long (Figure 7A, [30]). They are asymmetric in cross-section and appear as channel belts in the same way as those in siliciclastic depositional systems (e.g., fluvial channel, distributary channel). Channel bases are highly erosive with abundant burrows and few diagenetic modifications. High-energy rudstones, grainstones, and packstones fill the channels interbedding with finer grained carbonates or mudstones. Tidal channels of the Natih Formation outcrops are considered as resulting from tidal backfilling and accretion in tidal creek depositional systems during the transgressive phase [30]. In addition, the three-dimensional seismic azimuth map of the top Natih-e seismic reflector also clearly depicts the channel incisions and channel belt geometry in plane-view with a dimension of more than 1km wide and 30 km long (Figure 7B, [22]). A modern carbonate tidal channel analog of Joulters shoal north of Andros Island on the Great Bahama Bank displays the channel-belt geometry in plane-view (Figure 7C, [42]). For each channel, a main trunk channel is associated with several bifurcating smaller channels, no wash-over fans exit on the seaward side or the lagoonal side. A total of 43 tidal channels are recognized, the mean channel width is c.a. 0.83 km, and the mean channel length is c.a. 5.33 km (calculated based on total channel length of 229 km).

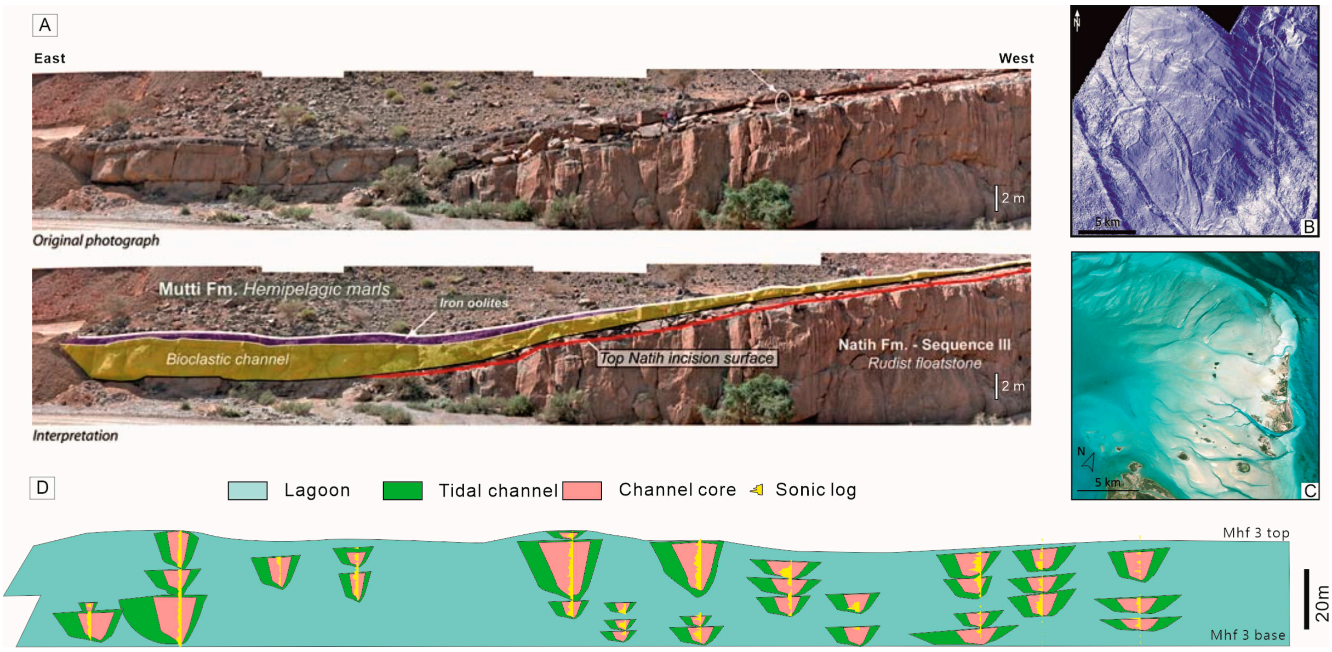

Figure 7. Characteristics of tidal channels. (**A**) Channels at the top of the Natih Formation showing erosion into rudist floatstone, modified from [10]; (**B**) Azimuth map of the top Natih-e seismic reflector showing geometries and incisions of tidal channels, modified from [22]; (**C**) Satellite image of modern analog tidal channels in Great Bahama Bank, taken from [42]; (**D**) Tidal channels interpreted in this study within Mhf 2 to Mhf 3.

In the present study, the tidal channel is identified based on cores and well logs. Within the entire Mishrif Formation, tidal channels are the only depositional unit characterized with apparent cross-lamination (Figures 2 and 8). Wavy, planer muddy laminations appear within grainstone–packstones and faint herringbone bi-directional cross-lamination could be identified in cores. Grains are generally well-sorted, with the appearance of re-worked millimeter-scale rudistid fragments (Figures 2 and 3), suggesting a high-energy condition. On a vertical profile, a “channeling-upward” (Figure 8) pattern is featured by, from base to top, (1) an irregular, erosive base with burrows; (2) grainstone–packstone with abundant bioclastic debris with intercalated thin wackestone–mudstones; (3) a plane, finer grained (wackestone–mudstone) top draping. This pattern is also captured on wireline logs, with a blocky-funnel upward-increase in gamma rays, blocky upward-decrease in sonic logs; the reservoir potential of tidal channels is well reflected by resistivity logs (Figures 4, 6 and 8).

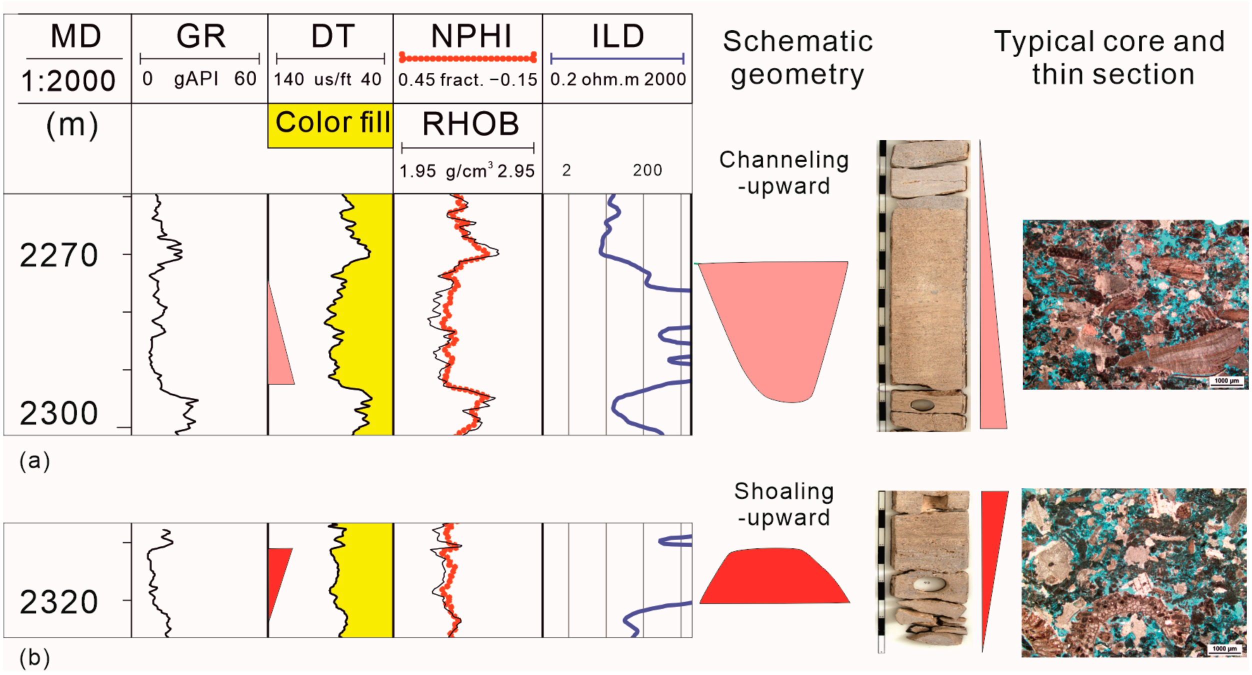

Figure 8. Features of (**a**) channeling-upward pattern and (**b**) shoaling-upward pattern on wireline logs, cores, and thin sections.

It is noteworthy that within a general channel-upward pattern, thin fine-grained intervals with less reservoir potential also occur, separating several thinner channeling-upward cycles. This might be interpreted as hierarchically smaller-scale units. In addition, a proper characterization of the internal channel architecture determines the remaining oil distribution and thus impacts the injection plan [10,22,43]. However, meter-scale heterogeneity is beyond the scope of this study and will be analyzed given more available cores and three-dimensional seismic data.

In the Arabian Plate, lithologies and biofacies generally match well to log data [3]; therefore, the log-based correlation undertaken in this study (Figures 4, 6 and 7D) allows a semi-quantitative characterization of geometrical parameters of tidal channels. In particular, tidal channel depth can be best identified by a "channeling-upward"/decrease-upward pattern based on the sonic logs. Widths of tidal channels cannot be easily measured and thus are not used in this study; three-dimensional seismic surveys are required to do so. In addition, the extension direction of tidal channels is supposed to be southwest–northeast, causing additional difficulty in the accurate measurement of tidal width, given the cross-section is in the north–south direction. A compilation of the 32 tidal channels (Figure 7D) in the study area suggest that minimum depth, maximum depth, and mean depth of tidal channel are 3.27, 22.67, and 8.93, respectively (Figure 9). The mean depth is similar to that of the Natih Formation outcrops as described by [30], with most of the channels having a depth c.a. 5 m. It should be noted that a few tidal channels are deeper than 20 m, this is perhaps due to an amalgamation of multiple smaller tidal channels, as demonstrated by the serrated motif of sonic logs, suggesting high-energy conditions of the tidal channels.

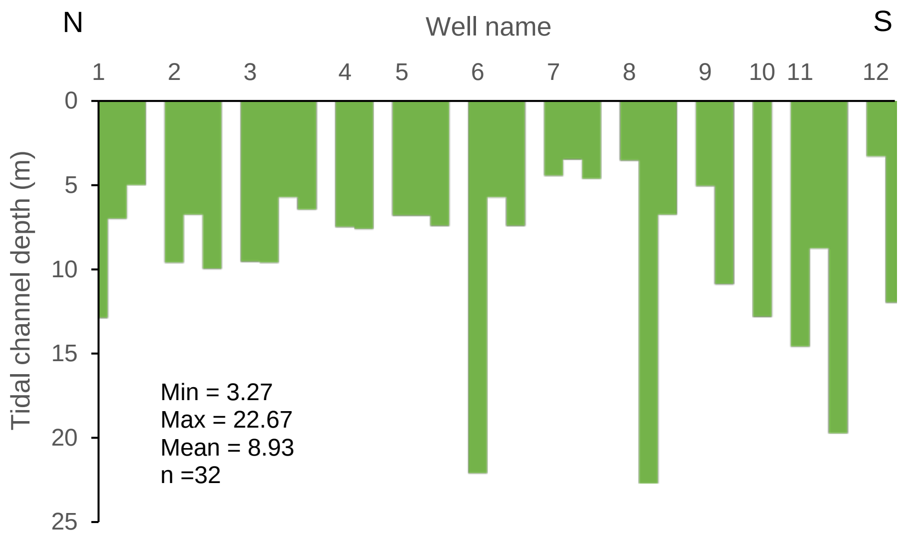

Figure 9. Compilation of tidal channel depth in the study area. X axis is the 12 wells encountering tidal channels from north to south.

In plane-view, tidal channels within carbonate-dominated ramps display a channelized feature similar to those fluvial meandering channels, as demonstrated by the modern sedimentology of the Great Bahama Bank "https://www.beg.utexas.edu/lmod/_IOL-CM01/cm01-step02b.htm (accessed on 1 May 2023)", courtesy of University of Texas at Austin, and the outcrop characterization of carbonate ramps in the Arabian Plate [30]. However, the plane-view of modern analogs and three-dimensional seismic slices both suggest that carbonate tidal channels appear relatively straight and less sinuous than meandering channels of siliciclastic systems (e.g., fluvial, delta).

5.2. Intra-Shelf Basin

Deposition of the Cenomanian–Turonian carbonates has been considered to occur on an extensive platform across the Arabian Plate, associated with an intra-shelf basin (the Najaf basin, or Rumaila basin, by [1]). High-resolution outcrop studies and seismic characterizations both proved that clinoform geobodies prograded towards the intra-shelf basin during relative sea level drops on the Arabian Plate [10,22,24,38]. The Najaf intra-shelf basin started to develop in the Early Cenomanian, southwest of the study area, partly controlled by faulting in the East Baghdad area [1]. Correspondingly, the Mishrif Formation is thinning towards the intra-shelf basin towards the southwest. During the late stage of the Mishrif deposition, the region between the Rumaila field and Zubair field was dominated by restricted lagoonal facies [33], and sub-basinal facies were developed west of the Rumaila field.

The correlation of wells at the middle region of the study area shows that in the sequence Mhf 4, bioclastic build-ups/shoal facies within lagoonal background gradually transits into mid-ramp of shallow marine facies (Figure 10A). Sub-basinal shales started to appear on top of the Mhf 4, between W16 and W18, suggesting the first occurrence of intra-shelf basin deposition (Figure 4). Consequently, it leads to a specific juxtaposition of shoal, lagoon, and sub-basinal shales (Figure 10A) with lagoonal-shoal facies directly grading into intra-shelfal facies, demonstrating an abrupt topographical break. Such an interpretation in this study has been confirmed by high-resolution outcrop characterizations of the Savark Formation (time-equivalent with the Mishrif Formation) in Iran (Figure 10B) by [11,30]. The layered organic-rich mudstones within the intra-shelf basin differentiate themselves from the underlying wackestones of lagoonal facies and the overlying ~80 m thick grainstone shoal (Figure 10B).

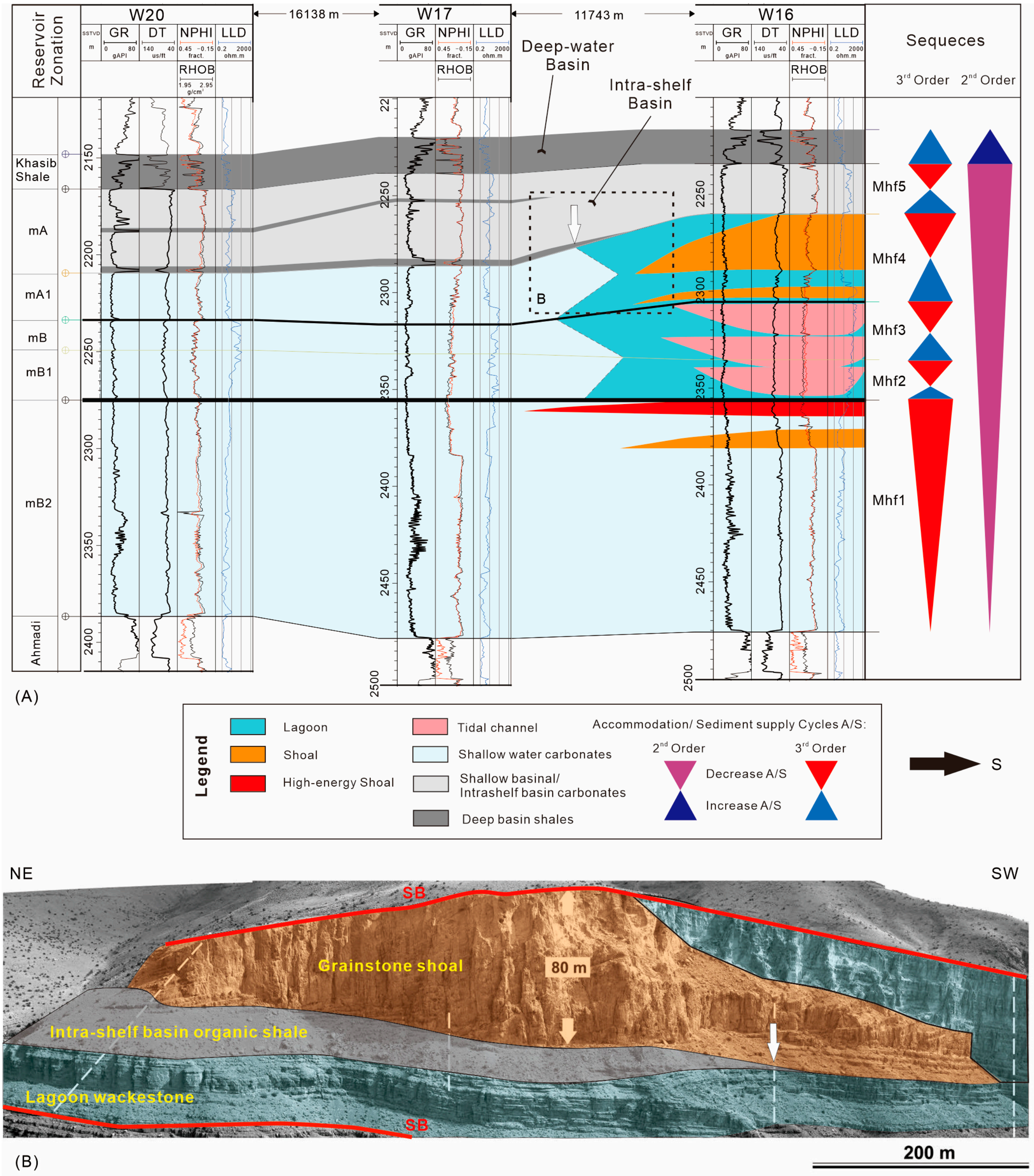

Figure 10. (**A**) Correlation of W16, W17, and W20 showing the stacking characteristics of lagoon, shoal, shallow-marine, and intra-shelf basin facies; see Figure 4 for detailed location of wells; (**B**) Outcrop of the Savark Formation in Iran showing similar stacking of grainstone shoal, lagoon wackestone, and intra-platform basin organic shales, modified from [30].

The development of this intra-shelf basin started in the upper part of the Mishrif Formation (Mhf 4 and Mhf 5) and significantly changed their depositional pattern. The intra-shelf basin changed the paleo-bathymetry such that the increase in accommodation space exceeded carbonate production. Consequently, organic-rich shales were deposited, perhaps consistent with the global anoxic event OAE2 (Oceanic Anoxic Event) at the Cenomanian–Turonian boundary [4], which is time-equivalent with the top Savark Formation within Zagros area [30] and the Natih Formation in Oman [10]. By contrast, the high-energy bioclastic grainstone shoal continued to develop in the platform northwards. When carbonate production exceeds the increasing rate of accommodation space, carbonate clinoforms are estimated to develop along the paleogeography between the platform and the intra-shelf basin. Small-scale bioclastic build-ups are locally developed on the platform margin (Figure 4). The Arabian Plate was characterized by a system whereby carbonate system production generally could not exceed the sea level rise [4,17]. On the flat ramp site, during the transgressive phase, grainstone shoals maintain aggradation, gradually giving rise to a steep topography. The increase in rate of sea-level gradually triggered the change from flat platform to intra-shelf basin via the steepening margin. In fact, sea level change is considered as the main controlling factor for the formation of the ramp–intrashelf depositional system. During different geological periods in the Arabian Plate, other three main intra-shelf basins were developed: the Early Jurassic Marrat intra-shelf basin, the Late Jurassic Hanifa intra-shelf basin, and the Aptian Bab intra-shelf basin; they were all triggered by a similar mechanism [4,17,24].

In the study area, the tectonic movement might also influence the deposition of the Mishrif Formation. A series of north–south trend dome/anticline was formed perhaps due to growing salt structure. Rudistid build-ups aggraded on the crest of dome. High paleotopography could result in erosion and the reworking of the rudistid build-ups which are then transported and dispersed into bioclastic grainstone shoals, similar to "tabular reefs" of several kms wide due to the uplift described by [33]. Such bioclastic build-ups are likely to develop on the flanks of anticlines following the down-dip paleogeography [9] and grade into the intra-shelf basin. In addition, because of the erosion and reworking, true rudistid reefs (framestones, floatstones, and boundstones) are rarely encountered [9].

5.3. Tectonic Influence on Shoal Complexes

Eustatic-level changes clearly exert control on the development of sequence stratigraphy and carbonate facies, as demonstrated earlier. Meanwhile, tectonic movements such as the salt movement and reactivation of basement faults, might happen at the same time with the deposition of rudist build-ups and hence influenced their development and distribution [35]. Being influenced by synchronous basement tectonics, regional studies suggest that the Mishrif Formation has undergone a general change from carbonate ramps in the early Cretaceous into rimmed shelves in middle-late Cretaceous [1,35]. The initiation of the Mishrif Formation was considered as being progradational onto sub-basinal facies towards the northeastern and southwestern direction [1,35]. In the study area, five progradational shoal complexes are interpreted within the Mhf 1 on a north–south cross section which is roughly parallel with the boundary of the Mishrif shallow marine facies and sub-basinal Rumaila/Ahmadi facies (Figure 1A). Consequently, shoals tend to develop in parallel along the platform margins; therefore, this could perhaps interpret why no isolated, localized, small-size build-ups/shoal are recognized in the cross section. Furthermore, the north–south prograding shoals happen to follow the hinge of a large anticline (Rumaila anticline). Therefore, the influence of the Infracambrian Hormuz Salt and the Samarra-Dujaila-Amara paleohighs also cannot be excluded [3,4]. The growing anticlines are favorable locations for developing rudist build-ups as they kept growing until they reached wave base and underwent erosion and reworking. Reworked rudist fragments were then dispersed into grainstone/packstone and formed "tabular reefs" or banks which are several kilometers wide [9,33]; thus, shoal complexes recognized within the Mhf 1 are likely "tabular reefs". South of the anticline in the study area, shoal complexes grade into deeper marine facies, suggesting the appearance of intra-shelf basin and quiescence of tectonic movements.

5.4. Sequence Stratigraphy within a Regional Framework

There are many previous studies on the sequence stratigraphy of the Mishrif Formation in southern Iraq and division of large-order sequences are widely agreed upon (e.g., megasequence AP8, supersequence IV). Smaller-order sequences, however, may vary depending on different types and availability of data used in their work. The classification of three third-order sequences for the Mishrif Formation has been widely applied regionally [3,24,30]. However, it can vary for different fields, even close-distance fields. For example, three third-order sequences are interpreted for W field [18], five third-order (or equivalent) sequences are interpreted for the R field [19,44], whereas six third-order (or equivalent) sequences are interpreted for the H field [6,18]. For formations equivalent to the Mishrif Formation in the Arabian Plate, different sequence stratigraphic frameworks also exist. For the Savark Formation in Iraq, four sequences, namely Sequence I-IV, are interpreted [30,45]. For the Natih Formation in Oman, five sequences, namely Sequence 1–5, are interpreted [11].

In addition, recognition of maximum flooding surfaces is also subjective according to different authors. MFS K120 and K140 are regionally comparable, represented by Ahmadi shales and Khasib shales, respectively [1,17]. The "disconformity" of the S2 top with significant exposure features by [3] is probably comparable, it is mostly likely the top of Mhf 1 in this study, and it is almost certainly the top of SB-D in the H field [6]. In the study area, K130 lies within Mhf 1, K135 is probably the maximum flooding surface of Mhf 2, and K140 is likely the maximum flooding surface of Mhf 5. Since no biostratigraphic analysis is applied, uncertainties associated with the interpretation of maximum flooding surfaces should be noted. Nevertheless, the stratigraphic framework proposed herein can help unravel reservoir zonation and compartmentalization in the study area, where each sequence is characterized by a specific facies association and is highly recognizable. The sequences are correlatable in the entire study area of several 10 s of km long.

5.5. Reservoir Architecture and Petroleum Potential

Depositional textures of carbonates of the Mishrif Formation have been significantly overprinted by diagenetic processes [3,8,20,39]. Reservoir zonation and heterogeneity are thus an integrated product of deposition and diagenesis. Detailed discussion on the diagenesis is beyond the scope of the current work and will be discussed in another independent study. Within the sequence stratigraphic framework, reservoir zonation is divided into mB2, mB1, mB, mA1, and mA, roughly corresponding to Mhf 1, Mhf 2, Mhf 3, Mhf 4, and Mhf 5, respectively (Figures 2 and 11). Depositional heterogeneities are briefly classified into the following four types.

5.5.1. High-Permeability Zones

Two types of high-permeability zones (permeability of 100 s mD in Figure 11) are recognized: shoal complexes at the top of mB2, and tidal channel within mB1 and mB. The former was developed at the latest regressive stage of the Mhf 1. After their deposition, the sequence boundary of Mhf 1 is accompanied by the first platform exposure of the Mishrif Formation. Diagenesis for this interval is prominent meteoric dissolution, creating dissolution pores and significantly improving reservoir quality. The latter was developed within the Mhf 2 and Mhf 3 (mB 1 and mB). The cross-section shows that grainstone tidal channels are frequently developed but few of them are mutually connected, instead, they form "isolated" high-K zones (Figure 4). Within the Mishrif Formation, these high-permeability zones generally form "thief zones" which represent more rapid water breakthroughs to production wells than predicted by flow simulations. These are of critical importance for reservoir performance; future studies should focus on unraveling their distribution in 3D space.

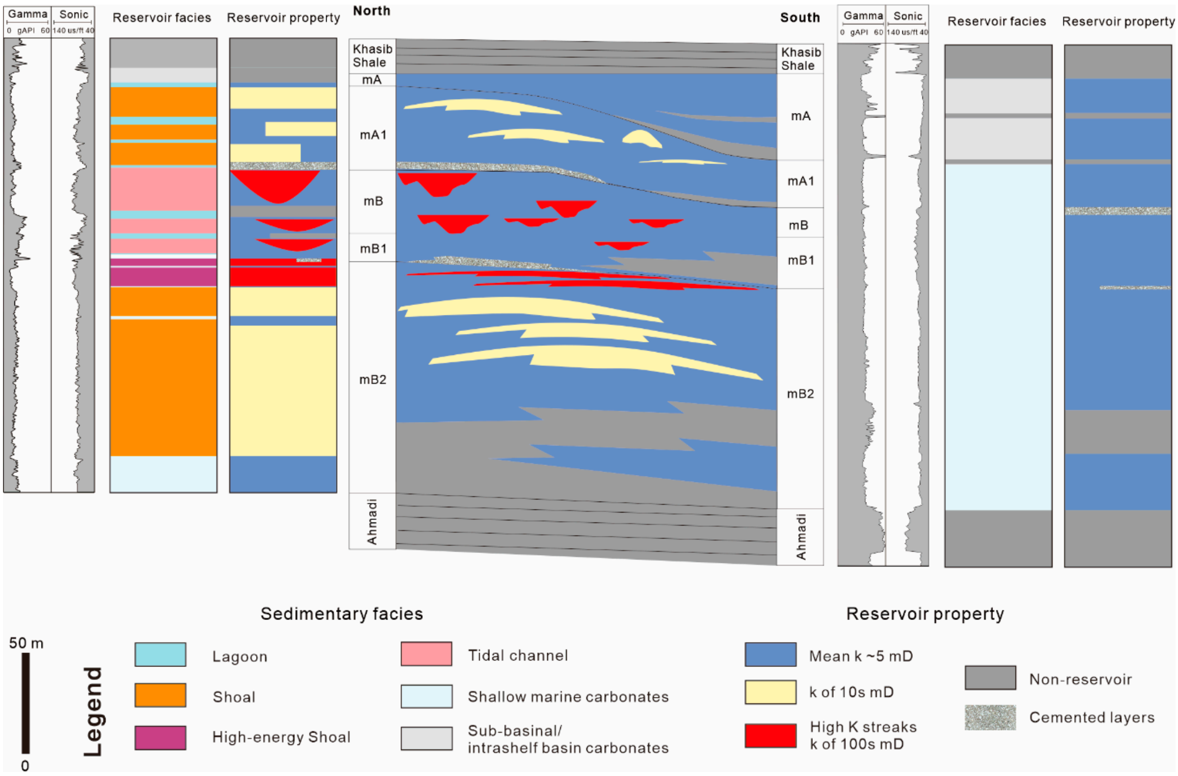

Figure 11. Schematic model showing reservoir zonation of the Mishrif Formation from north to south. Sedimentary facies and reservoir property are highlighted independently.

5.5.2. Medium-Permeability Layers

These layers have permeability of 10 s mD, including prograding shoal complex in mB2, isolated shoals and mounds in mA1. The regressive cycle of the Mhf 1 constitutes several progradational shoal complexes enveloped within a low-K background (Figures 4 and 11), suggesting continuous decrease in A/S ratio. Due to good lateral continuity and connectivity, they also represent decent reservoir potential. Within mA1, grainstones within laterally continuous shoals and more isolated mounds also have reservoir potential.

5.5.3. Intra-Reservoir Baffles

Micro-porous baffles appear within mB2, mB1, and mA (non-reservoir in Figure 11). Baffles in mB2 are likely equivalent to wackestones/marls of the Rumaila Formation, where a single thick layer in the north "splits" into two individual layers southwards. At the basal part of mB1, a thick lagoonal wackestone baffle prominently occurs in the southern region. At the boundary of mA and mB, the sequence boundary of Mhf 4 (mB) was accompanied by heavy cementation in the north and mudstone in the south, reflected by high gamma-ray values. In mA, the thin tidal wackestone layer becomes two thick and laterally extensive sub-basinal mudstones southwards.

5.5.4. Inter-Reservoir/Regional Barriers

The Mishrif Formation was encased by two regional barriers of thick basinal shales with overlying Khasib Formation and underlying Ahmadi Formation; the Khasib shales are seals for the Mishrif Formation. Fabrics of shales might impact the residual oil distribution in the reservoir [35,36], however, it is beyond the scope of the current work.

The study area is characterized by a general deepening-south pattern. Gamma-ray values are generally higher while sonic values are generally lower in south (Figure 11). A generally lower reservoir potential is therefore predicted, despite the development of local high-K build-ups in the south.

6. Conclusions

Five types of facies associations are classified for the Mishrif reservoir in south Iraq: lagoon, shoal, rudist bioherm, shallow marine, and deep marine. Such a classification allows convenient differentiation and interpretation on wireline logs, and could be applied in carbonate reservoir exploration and development for other areas in the Arabian Plate.

The Mishrif reservoir is divided into five third-order sequences from Mhf 1 to Mhf 5. Sea level changes exert clear control on the depositional evolution. When the Mishrif Formation deposition was initiated after transition from Ahmadi shales, a shallow marine environment was prominent. Clinoform-like progradational shoal complexes are identified within the regressive cycle of Mhf 1, in response to continuous sea level fall. Mhf 2 to Mhf 3 are dominated by lagoonal system, encasing tidal channels and subordinate mounds. Sea level rise in Mhf 4 created shallow marine environment allows the final development phase of shoal complexes. Mhf 5 is dominated by marine environment and becomes deeper southwards.

The Rumaila/Najaf intra-shelf basin was initiated in the late stage of Mhf 4. The thickness of Mhf 5 increased significantly towards the south, multiple thick mudstones were developed within the intra-shelf basin, suggesting that the intra-shelf basin was perhaps maturely developed at this stage. Reservoir characteristics of the Mishrif Formation, especially the upper part, were significantly controlled by the development of intra-shelf basin.

The reservoir zonation of the Mishrif Formation is a combined product of deposition and diagenesis. Five reservoir zones including mB2, mB1, mB, mA1, and mA, are recognized, roughly corresponding to five third-order sequences. Two main reservoir units are recognized: shoal complexes at the top of mB2, and tidal channel within mB1 and mB. They are both dominated by grainstones and highly permeable zones, but display different "shoaling-upward" and "channeling-upward" patterns, respectively. The reservoir quality of the former is further enhanced by meteoric dissolution due to subaerial exposure at the sequence boundary. Tidal channels appear "isolated" with limited inter-connectivity, they can form "thief zones" which represent faster water breakthroughs to production wells than predicted by flow simulations and are of critical importance for reservoir performance. High-resolution seismic mapping in the future will help better capture the geometry and distribution of shoal and channel geobodies.

Author Contributions: Conceptualization, W.Z. and Y.L.; methodology, W.Z.; software, D.L., Y.D., J.X., and Y.W.; validation, L.Z.; data curation, Y.W. and B.S.; writing—original draft preparation, L.Z.; writing—review and editing, L.Z. and B.S.; supervision, Y.L.; project administration, B.S.; funding acquisition, B.S. All authors have read and agreed to the published version of the manuscript.

Funding: This research was funded by PETROCHINA, grant number 2017ZX05030-001, 2021DQ0407 and 2021DJ3202.

Institutional Review Board Statement: Not applicable.

Informed Consent Statement: Not applicable.

Data Availability Statement: Not applicable.

Acknowledgments: Jiquan Yin, Mingsheng Feng and Guangya Zhu from RIPED are thanked for their insightful discussions. PETROCHINA is thanked for access to the data and permission to publish.

Conflicts of Interest: The authors declare no conflict of interest.

References

1. Aqrawi, A.; Mahdi, T.; Sherwani, G.; Horbury, A. Characterisation of the Mid-Cretaceous Mishrif reservoir of the southern Mesopotamian Basin, Iraq. In Proceedings of the American Association of Petroleum Geologists Conference and Exhibition, Manama, Bahrain, 7–10 March 2010; pp. 7–10.
2. Al-Mimar, H.S.; Awadh, S.M.; Al-Yaseri, A.A.; Yaseen, Z.M. Sedimentary units-layering system and depositional model of the carbonate Mishrif reservoir in Rumaila oilfield, Southern Iraq. *Model. Earth Syst. Environ.* **2018**, *4*, 1449–1465. [CrossRef]
3. Mahdi, T.A.; Aqrawi, A.A.; Horbury, A.D.; Sherwani, G.H. Sedimentological characterization of the mid-Cretaceous Mishrif reservoir in southern Mesopotamian Basin, Iraq. *Geoarabia* **2013**, *18*, 139–174. [CrossRef]

4. Sharland, P.R.; Casey, D.M.; Davies, R.B.; Simmons, M.D.; Sutcliffe, O.E. Arabian Plate Sequence Stratigraphy—Revisions to SP2. *Geoarabia* **2004**, *9*, 199–214. [CrossRef]
5. Simmons, M.D.; Sharland, P.R.; Casey, D.M.; Davies, R.B.; Sutcliffe, O.E. Arabian Plate sequence stratigraphy: Potential implications for global chronostratigraphy. *Geoarabia* **2007**, *12*, 101–130. [CrossRef]
6. Cantrell, D.; Shah, R.; Ou, J.; Xu, C.; Phillips, C.; Li, X.; Hu, T. Depositional and diagenetic controls on reservoir quality: Example from the upper Cretaceous Mishrif Formation of Iraq. *Mar. Pet. Geol.* **2020**, *118*, 104415. [CrossRef]
7. Ismail, M.J.; Ettensohn, F.R.; Handhal, A.M.; Al-Abadi, A.M. Facies analysis of the Middle Cretaceous Mishrif Formation in southern Iraq borehole image logs and core thin-sections as a tool. *Mar. Pet. Geol.* **2021**, *133*, 105324. [CrossRef]
8. Mahdi, T.; Aqrawi, A. Sequence stratigraphic analysis of the mid-Cretaceous Mishrif Formation, southern Mesopotamian Basin, Iraq. *J. Pet. Geol.* **2014**, *37*, 287–312. [CrossRef]
9. Sadooni, F.N. The nature and origin of Upper Cretaceous basin-margin rudist buildups of the Mesopotamian Basin, southern Iraq, with consideration of possible hydrocarbon stratigraphic entrapment. *Cretac. Res.* **2005**, *26*, 213–224. [CrossRef]
10. Gréland, C.; Razin, P.; Homewood, P. Channelized systems in an inner carbonate platform setting: Differentiation between incisions and tidal channels (Natih Formation, Late Cretaceous, Oman). *Geol. Soc. Lond. Spéc. Publ.* **2010**, *329*, 163–186. [CrossRef]
11. Razin, P.; Grélaud, C.; van Buchem, F. The mid-Cretaceous Natih Formation in Oman: A model for carbonate platforms and organic-rich intrashelf basins. *AAPG Bull.* **2017**, *101*, 515–522. [CrossRef]
12. Alsharhan, A.S. Facies Variation, Diagenesis, and Exploration Potential of the Cretaceous Rudist-Bearing Carbonates of the Arabian Gulf1. *AAPG Bull.* **1995**, *79*, 531–550.
13. Alsharhan, A.S.; Kendall, C.G.S.C. Paleozoic sequence stratigraphy, depositional systems, and hydrocarbon habitats across the Arabian plate. *AAPG Bull.* **2021**, *105*, 1149–1198. [CrossRef]
14. Mahdi, T.A.; Aqrawi, A.A.M. Role of facies diversity and cyclicity on the reservoir quality of the mid-Cretaceous Mishrif Formation in the southern Mesopotamian Basin, Iraq. *Geol. Soc. Lond. Spéc. Publ.* **2017**, *435*, 85–105. [CrossRef]
15. Aqrawi, A.A.M.; Thehni, G.A.; Sherwani, G.H.; Kareem, B.M.A. Mid-Cretaceous rudist-bearing carbonates of the Mishrif Formation: An important reservoir sequence in the Mesopotamian Basin, Iraq. *J. Pet. Geol.* **1998**, *21*, 57–82. [CrossRef]
16. Reulet, J. Carbonate reservoir in a marine shelf sequence, Mishrif Formation, Cretaceous of the Middle East. In *Exploration for Carbonate Petroleum Reservoirs. Elf Aquitaine*; John Wiley and Sons: New York, NY, USA, 1982; pp. 165–173.
17. Sharland, P.; Archer, R.; Casey, D.; Davies, R.; Hall, S.; Heward, A.; Horbury, A.; Simmons, M. Sequence stratigraphy of the Arabian Plate. *GeoArabia* **2001**, *2*, 1.
18. Deng, H.; Fu, M.; Huang, T.; Gluyas, J.G.; Tong, M.; Wang, X.; Zhou, W.; Liu, F. Ahdeb oil field, Mesopotamian Basin, Iraq: Reservoir architecture and oil charge history. *AAPG Bull.* **2018**, *102*, 2447–2480. [CrossRef]
19. Lehmann, C.; Ryder, K.; Disimone, S.; Perrotta, S. Sedimentology and Sequence Stratigraphy of the Mishrif Formation and it's Impact on Reservoir Heterogeniety, Rumaila Field, Southern Iraq. In Proceedings of the Second EAGE workshop on Iraq, Dead Sea, Jordan, 15–18 September 2013; p. 355. [CrossRef]
20. Zhong, Y.; Zhou, L.; Tan, X.; Guo, R.; Zhao, L.; Li, F.; Jin, Z.; Chen, Y. Characteristics of depositional environment and evolution of Upper Cretaceous Mishrif Formation, Halfaya Oil field, Iraq based on sedimentary microfacies analysis. *J. Afr. Earth Sci.* **2018**, *140*, 151–168. [CrossRef]
21. Adams, E.W.; Grélaud, C.; Pal, M.; Csoma, A.; Al Ja'Aidi, O.S.; Al Hinai, R. Improving reservoir models of Cretaceous carbonates with digital outcrop modelling (Jabal Madmar, Oman): Static modelling and simulating clinoforms. *Pet. Geosci.* **2011**, *17*, 309–332. [CrossRef]
22. Droste, H.; Buchem, F.S.P.V.; Gerdes, K.D.; Esteban, M. High-resolution seismic stratigraphy of the Shu'aiba and Natih formations in the Sultanate of Oman: Implications for Cretaceous epeiric carbonate platform systems. In *Mesozoic and Cenozoic Carbonate Systems of the Mediterranean and the Middle East: Stratigraphic and Diagenetic Reference Models*; Geological Society of London: London, UK, 2010; Volume 329, pp. 145–162.
23. Grélaud, C.; Razin, P.; Homewood, P.W.; Schwab, A.M. Development of Incisions on a Periodically Emergent Carbonate Platform (Natih Formation, Late Cretaceous, Oman). *J. Sediment. Res.* **2006**, *76*, 647–669. [CrossRef]
24. van Buchem, F.S.P.; Razin, P.; Homewood, P.W.; Oterdoom, W.H.; Philip, J. Stratigraphic Organization of Carbonate Ramps and Organic-Rich Intrashelf Basins: Natih Formation (Middle Cretaceous) of Northern Oman. *AAPG Bull.* **2002**, *86*, 21–53.
25. Iraji, S.; Soltanmohammadi, R.; De Almeida, T.R.; Munoz, E.R.; Basso, M.; Vidal, A.C. Laboratory and Numerical Examination of Oil Recovery in Brazilian Pre-salt Analogues Based on CT images. In Proceedings of the Third EAGE Conference on Pre Salt Reservoirs, Rio de Janeiro, Brazil, 23–25 November 2022; Volume 2022, pp. 1–6.
26. Iraji, S.; Soltanmohammadi, R.; Munoz, E.R.; Basso, M.; Vidal, A.C. Core scale investigation of fluid flow in the heterogeneous porous media based on X-ray computed tomography images: Upscaling and history matching approaches. *Geoenergy Sci. Eng.* **2023**, *225*, 211716. [CrossRef]
27. Ahmed, B.; Bakht, S.; Wahid, S.; Hanif, M. Structural Analysis and Reservoir Characterisation of Cretaceous Sequence in Kohala Bala, Khyber Pakhtunkhwa, Pakistan. *Rud. Zb.* **2022**, *37*, 65–81. [CrossRef]
28. Pitman, J.K.; Steinshouer, D.; Lewan, M.D. Petroleum generation and migration in the Mesopotamian Basin and Zagros Fold Belt of Iraq: Results from a basin-modeling study. *Geoarabia* **2004**, *9*, 41–72. [CrossRef]
29. Chatton, M.; Hart, E. *Announcement of a Rock Unit Redefined. Ratawi Formation: Iraq Petroleum Company Unpublished Report*; Oil Exploration Company Archive: Baghdad, Iraq, 1962.

30. Razin, P.; Taati, F.; Van Buchem, F. Sequence stratigraphy of Cenomanian–Turonian carbonate platform margins (Sarvak Formation) in the High Zagros, SW Iran: An outcrop reference model for the Arabian Plate. *Geol. Soc. Lond. Spec. Publ.* **2010**, *329*, 187–218. [CrossRef]
31. Dunham, R.J. *Classification of Carbonate Rocks According to Depositional Textures*; American Association of Petroleum Geologists: Tulsa, OK, USA, 1962; Volume 38, pp. 108–121.
32. Embry, A. Transgressive–regressive (T–R) sequence analysis of the Jurassic succession of the Sverdrup Basin, Canadian Arctic Archipelago. *Can. J. Earth Sci.* **1993**, *30*, 301–320. [CrossRef]
33. Gaddo, J. The Mishrif Formation paleoenvironment in the Rumaila/Tuba/Zubair region of South Iraq. *J. Geol. Soc. Iraq* **1971**, *4*, 1–12.
34. Aqrawi, A.A.; Goff, J.C.; Horbury, A.D.; Sadooni, F.N. *The petroleum Geology of Iraq*; Scientific Press: Beaconsfield, UK, 2010.
35. Sadooni, F.; Aqrawi, A.; Sadooni, F.; Aqrawi, A. Cretaceous Sequence Stratigraphy and Petroleum Potential of the Mesopotamian Basin, Iraq. In *Middle East Models of Jurassic-Cretaceous Carbonate Systems*; Alsharhan, A., Scott, B., Eds.; SEPM Special Publication: Tulsa, OK, USA, 2000.
36. Meng, M.; Ge, H.; Shen, Y.; Ji, W.; Li, Z. Insight into Water Occurrence and Pore Size Distribution by Nuclear Magnetic Resonance in Marine Shale Reservoirs, Southern China. *Energy Fuels* **2022**, *37*, 319–327. [CrossRef]
37. Meng, M.; Peng, J.; Ge, H.; Ji, W.; Li, X.; Wang, Q. Rock Fabric of Lacustrine Shale and Its Influence on Residual Oil Distribution in the Upper Cretaceous Qingshankou Formation, Songliao Basin. *Energy Fuels* **2023**, *37*, 7151–7160. [CrossRef]
38. van Buchem, F.S.P.; Simmons, M.D.; Droste, H.J.; Davies, R.B. Late Aptian to Turonian stratigraphy of the eastern Arabian Plate—Depositional sequences and lithostratigraphic nomenclature. *Pet. Geosci.* **2011**, *17*, 211–222. [CrossRef]
39. Zhang, L.; Li, R.; Deng, H.; Fu, M.; Hu, L.; Guo, X.; Xie, X.; Zhao, C. Identification, distribution characteristics, and effects on production of interlayers in carbonate reservoirs: A case study from the Cretaceous Mishrif Formation in Halfaya Oilfield, Iraq. *J. Pet. Sci. Eng.* **2021**, *202*, 108571. [CrossRef]
40. Hollis, C. Diagenetic controls on reservoir properties of carbonate successions within the Albian–Turonian of the Arabian Plate. *Pet. Geosci.* **2011**, *17*, 223–241. [CrossRef]
41. de Periere, M.D.; Durlet, C.; Vennin, E.; Caline, B.; Boichard, R.; Meyer, A. Influence of a major exposure surface on the development of microporous micritic limestones—Example of the Upper Mishrif Formation (Cenomanian) of the Middle East. *Sediment. Geol.* **2017**, *353*, 96–113. [CrossRef]
42. Purkis, S.J.; Harris, P. Quantitative interrogation of a fossilized carbonate sand body—The Pleistocene Miami oolite of South Florida. *Sedimentology* **2017**, *64*, 1439–1464. [CrossRef]
43. Wei, H.; Zhu, H.; Li, H.; Shi, S.; Gan, S.; Zhai, Z. The Study of the Reservoir Inter-architecture Structure and Remaining Oil in the Eastern Part of Sabei II District. *Rud. Geološko-Naft. Zb.* **2019**, *34*, 13–20. [CrossRef]
44. Al-Ali, M.; Mahdi, M.; Alali, R. Microfacies and depositional environment of Mishrif Formation, north Rumaila Oilfielfd, southern Iraq. *Iraqi Geol. J.* **2019**, *52*, 91–104.
45. Kiani, A.; Saberi, M.H.; ZareNezhad, B.; Mehmandosti, E.A. Reservoir zonation in the framework of sequence stratigraphy: A case study from Sarvak Formation, Abadan Plain, SW Iran. *J. Pet. Sci. Eng.* **2022**, *208*, 109560. [CrossRef]